

Stability Analysis of Contact Scanning Probe for Micro/Nano Coordinate Measuring Machine

LI Rui-jun^{1,2}, FAN Kuang-chao^{1,3}, QIAN Jian-zhao¹, HUANG Qiang-xian¹, GONG Wei¹, MIAO Jin-wei¹
(1. School of Instrument Science and Opto-Electric Engineering, Hefei University of Technology, Hefei 230009, China;
2. Department of Automation and Information Engineering, Anhui Electrical Engineering Professional Technique College,
Hefei 230051, China; 3. Department of Mechanical Engineering, National Taiwan University, Taipei 10617, China)

Abstract: The stability of a high accuracy contact scanning probe for micro/nano coordinate measuring machine (CMM) was analysed in this paper. This probe was composed of a fiber stylus with a ball tip, a mechanism with a wire-suspended floating plate, a two-dimensional (2D) angle sensor and a miniature Michelson linear interferometer. The stylus was attached to the floating plate. When a contact force was applied to the ball tip, the wires would experience elastic deformation and then the mirrors mounting on the plate would be tilted or displaced in vertical. The displacements of mirrors could be detected by 2D angle sensor and miniature Michelson linear interferometer. Experimental results show that the fluctuation of environmental temperature is the primary factor in affecting the stability of the probe. It is also found that the mechanical structure and components of the probe are much more sensitive to environmental temperature than the optical and electronic components of the probe. The probe can achieve the required resolution of 1 nm and the standard deviation of 30 nm as long as it is kept in a constant temperature chamber for at least 4 h before the measurement.

Keywords: stability; temperature drift; two-dimensional (2D) angle sensor; Michelson interferometer; micro/nano coordinate measuring machine (CMM)

微纳米三坐标测量机接触扫描探头稳定性分析

李瑞君^{1,2}, 范光照^{1,3}, 钱剑钊¹, 黄强先¹, 龚伟¹, 苗晋伟¹

(1. 合肥工业大学仪器科学与光电工程学院, 合肥 230009; 2. 安徽电气工程职业技术学院自动化与信息工程系, 合肥 230051; 3. 台湾大学机械工程学系, 台北 10617)

摘要: 对微纳米三坐标测量机(CMM)高精度扫描探头的稳定性进行了分析。该扫描探头由带有球头的光纤探针、悬浮机构、二维角度传感器和微型迈克尔逊干涉仪4部分组成。光纤探针和悬浮片固定在一起,当光纤探针的球头受到触碰时,会带动悬浮机构的悬线发生形变,进而导致贴在悬浮片上的平面反射镜倾斜或在竖直方向上发生位移,前者由二维角度传感器进行感测,后者由微型迈克尔逊干涉仪进行感测。实验结果表明,环境温度的变化是影响探头稳定性的主要因素,探头中机械结构和部件对温度变化的敏感性要远远大于探头中光电器件对温度变化的敏感性。只要将探头放到一个恒温箱中,待恒温箱温度稳定4h再开始测量,探头即可达到1nm的分辨力和30nm的测量标准差。

关键词: 稳定性; 温度漂移; 二维角度传感器; 迈克尔逊干涉仪; 微纳米三坐标测量机(CMM)

中图分类号: TP216 **文献标志码:** A **文章编号:** 1672-6030(2012)02-0125-07

收稿日期: 2011-09-22.

基金项目: 国家高技术研究发展计划(863计划)资助项目(2008AA042409);国家自然科学基金资助项目(50875073);安徽省教育厅高等学校优秀青年人才基金资助项目(2011SQRL179)。

作者简介: 李瑞君(1977—),男,讲师, liruijun001@126.com.

通讯作者: 范光照,教授, fan@ntu.edu.tw.

The increasing demands of industry for higher accuracy measurements of micro systems have led to the development of micro/nano dimensional metrology [1]. During the past decade, a variety of contact probe systems have been designed for micro/nano coordinate measuring machines (CMMs), such as silicon-based CMM [2], flexure structure-based CMM [3-4], fiber Bragg grating type CMM [5], boss membrane structures [6-7], suspension plate [8-40], single fiber [11] and vibrating mode [12-13] for touch triggering or touch scanning mode.

As a micro/nano measuring instrument, most of the contact probe systems need to obtain 1 nm resolution and less than 100 nm standard deviation [2-43]. The stability of the probe determines whether the probe can meet such a high requirement. For the scanning probe we have developed in this paper, the required resolution is 1 nm and the standard deviation is less than 30 nm. This probe was composed of a fiber stylus with a ball tip, a mechanism with a wire-suspended floating plate, a two-dimensional (2D) angle sensor modified from a DVD pick-up head and a miniature Michelson linear interferometer. The main factors in affecting the stability of the probe were experimentally investigated. The probe can meet its requirement.

1 Probe structure and principle

1.1 Probe structure

The developed contact scanning probe was composed of a fiber stylus with a ball tip, a mechanism with a wire-suspended floating plate, a 2D angle sensor modified from a DVD pick-up head, and a miniature Michelson linear interferometer, as shown in Fig. 1 and Fig. 2. The stylus was inserted to the floating plate, which was suspended by four evenly distributed wires connected to the supporting ring. The contact force caused the floating plate to tilt and moved as a rigid body while the wires experienced elastic deformations. The tilt of the floating plate was detected by the 2D angle sensor with respect to one of the four mirrors mounted at the ends of four arms, respectively. The other redundant mirrors were used for weight balance. The vertical displacement of the plate was detected by a miniature Michelson interferometer with respect to

the central mirror. Two fine adjusting flexure mechanisms were specially designed to fine tune the emitted angles of two laser beams from the angle sensor and the interferometer, respectively. With such a configuration the movement of the probe tip can be solved by three sensing signals (θ , φ and Δl) due to the contact force in X , Y and Z directions.

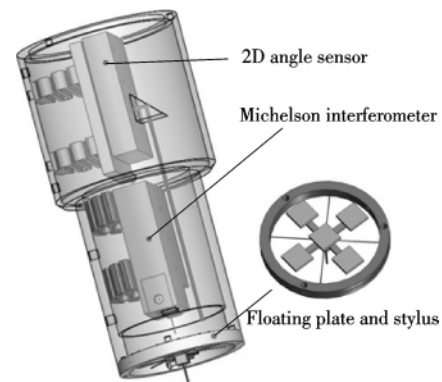


Fig. 1 Structure of the probe

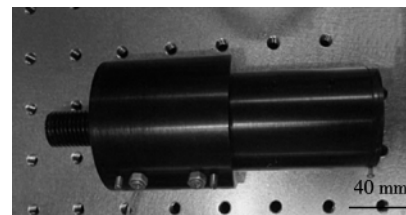


Fig. 2 Photograph of the probe

1.2 2D angle sensor

The schematic of the 2D angle sensor employed in this paper is shown in Fig. 3. It was modified from a DVD pick-up head (Hitachi HOP-1000) [8,14], which was inexpensive but adequately accurate. The original objective lens and the voice coil motor of the DVD pick-up head were removed so as to output with a collimated laser beam. Instead of the built-in four-quadrant photodiode (QPD), a QPD with a larger detecting area (1.3 mm × 2.5 mm) was used as the beam spot position detector. The collimated laser beam is projected onto the plane mirror. When the mirror normal is in line with the laser beam, the reflected laser beam is focused at the center of the QPD. A tilt of the plane mirror causes a corresponding lateral shift of the position of the focused light spot across the center of the QPD. The photo detector transforms the incident energy of the focused light spot into

current signals. Deviations of the focused light spot from the center of the photodiode result in a corresponding change in the magnitudes of the current signals output by the QPD. By applying an appropriate resistance to these electrical current signals, voltage signals (V_A , V_B , V_C and V_D) can be obtained. Changes in the magnitudes of these signals can then be used to determine the X - and Y -coordinates of the position of the focused light spot on the photodiode in accordance with the expressions:

$$X = k [(V_A + V_D) - (V_B + V_C)] \quad (1)$$

$$Y = k [(V_A + V_B) - (V_C + V_D)] \quad (2)$$

where k is the coefficient.

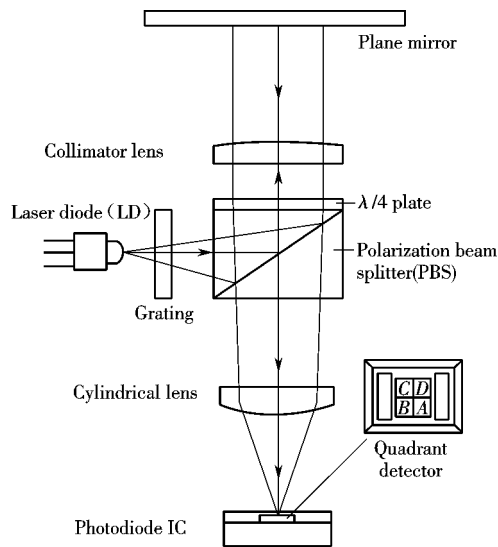


Fig. 3 Schematic of the 2D angle sensor

1.3 Michelson interferometer

Fig. 4 shows the schematic of a miniature Michelson interferometer designed for this paper. It is responsible for sensing of the Z -motion of the ball tip. The laser beam is separated into a S-beam and a P-beam by PBS1 with equal intensity. The P-beam passes through PBS1 and the S-beam is reflected to the reference mirror. The P-beam is changed to a right-circularly polarizing beam by the quarter wave plate (Q1) and reflected by the object mirror. When it passes through Q1 twice it is changed to a S-beam. Similarly, the reflected S-beam is changed to a P-beam when it passes through Q2 twice. These two returned beams will not go back to the LD but propagate to Q3, and then the P-beam changes to a right-circularly polarizing beam and the S-beam changes to a left-circularly polarizing beam. The NPBS splits both beams into

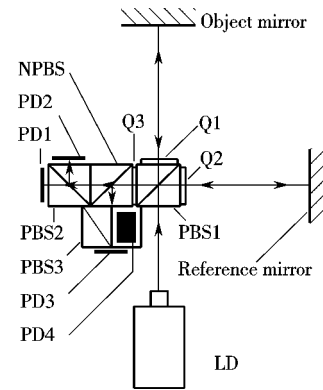


Fig. 4 Schematic of Michelson interferometer

two separate beams to PBS2 and PBS3 with equal intensity. PBS2 changes the left- and right-circularly polarizing beams from NPBS into two P-beams and two S-beams, which interfere with each other. PBS3 is placed along the direction of 45° with the NPBS. PBS3 also generates two P-beams and two S-beams interfering with each other. These four pairs of interfering beams are phase shifted into 0° , 90° , 180° and 270° by PBS2 and PBS3 (with fast axis set as 45°). The four photo detectors (PD1, PD2, PD3 and PD4) are used to detect the interference light separately. By using the Jones vector, the intensity of each photo detector can be expressed as^[15]

$$I_{PD1} = A [1 - \cos(2\Delta\omega t)] \quad (3)$$

$$I_{PD2} = A [1 + \cos(2\Delta\omega t)] \quad (4)$$

$$I_{PD3} = A [1 + \sin(2\Delta\omega t)] \quad (5)$$

$$I_{PD4} = A [1 - \sin(2\Delta\omega t)] \quad (6)$$

$$\Delta\omega = 4\pi \frac{\Delta l}{\lambda} \quad (7)$$

where I_{PD1} , I_{PD2} , I_{PD3} , I_{PD4} are the current intensities of the four photo detectors separately; A is the amplitude of the output of polarizing beams from Q3; Δl is the optical path difference between the reference beam and the object beam, which is the Z movement of the central mirror of the floating plate in the probe; λ is the wavelength of the LD; $\Delta\omega$ is the initial phase because Δl is not exactly a multiple of $\lambda/2$.

Regarding the signal processing, with the operation of $(I_{PD2} - I_{PD1})$ and $(I_{PD3} - I_{PD4})$, two orthogonal sinusoidal signals with $\pi/2$ phase shift can be obtained, as shown in Fig. 5. With the pulse counting and the phase subdivision techniques, the Z -motion of the object mirror can be resolved to nanometer resolution.

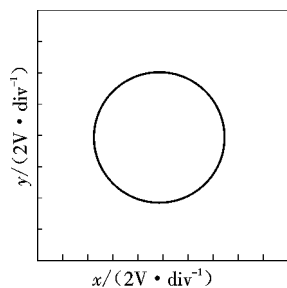


Fig.5 Normalized waveforms

2 Experiments and analysis

2.1 Experimental setup

The schematic of the experimental setup is shown in Fig.6. The workpiece is moved by a linear stage to approach the probe tip. After the contact position, the floating plate will be tilted about Y or X axis, respectively, when the workpiece motion is in the X or Y direction. The tilted angle can be sensed by the 2D angle sensor. If the motion is in Z direction, the floating plate will be pushed upward and the linear displacement can be sensed by the Michelson interferometer. Fig.7 shows the signal processing of the probe system. A constant temperature chamber^[16] is used to control the environment temperature, which is particularly made for the operating environment of the developed micro/nano CMM^[9], with in the stability of $(20 \pm 0.025)^\circ\text{C}$. Experiments within and without the temperature controlled environment are conducted with respect to each possible error source. Details are reported in the following sections.

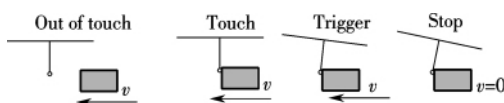


Fig.6 Schematic of experimental setup

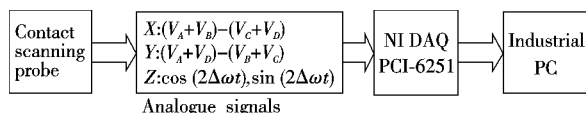


Fig.7 Signal processing of the probe system

2.2 Experiments of angle measurement system

2.2.1 Stability test and analysis

The angle measurement system is composed of an

angle sensor, a circuit board, fixing and adjusting mechanisms and reflection mirrors. First of all, these components are assembled together in the manner, as shown in Fig.1, and then the probe is connected with a data acquisition card (NI DAQ PCI-6251) and an industrial PC, as shown in Fig.7. Then, the probe is kept still and the two angle signals are acquired in the environment whose temperature is not controlled. Fig.8 shows the results of $(V_A + V_B - V_C - V_D)$, which drifts about 1.3 V within 2.5 h.

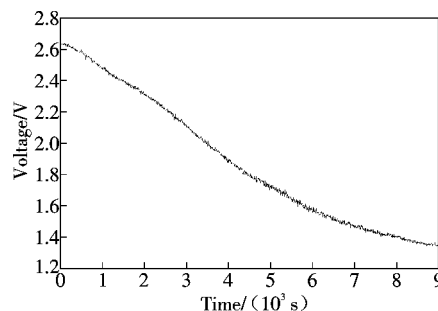


Fig.8 Result of the angle measurement system in ordinary environment

In order to investigate the error source of the stability, another experiment with this probe in a constant temperature chamber and with the same repeated procedure was carried out. The two angle signals are required after the temperature in the chamber is stable, i. e. , the temperature fluctuation range is less than 0.05°C , and the results are shown in Fig.9. It is seen that the total drift is only about 30 mV for the duration of 2.5 h.

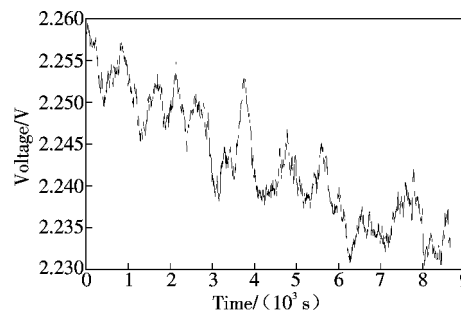


Fig.9 Result of the angle measurement system in the constant temperature chamber

From Fig. 8 and Fig. 9, it can be concluded that the drift of the angle measurement system is significantly influenced by temperature. Each part of the angle measurement system may be sensitive to temperature change,

such as the LD, the QPD, the circuit board and the mechanical components and structure. More experiments were carried out to investigate which part is playing the dominating role in leading to such a large drift.

First of all, the circuit board was tested. On this board there were four input ends that were corresponding to the four quadrant photocell sensors and two output ends ($V_A + V_B - V_C - V_D$ and $V_A + V_D - V_B - V_C$). In order to eliminate the influence caused by the LD and the QPD, four different voltage signals with the magnitudes equivalent to the four-quadrant's output from a precision power supply, were applied to the circuit. One of the output signals in ordinary environment is shown in Fig. 10, which indicates that the signal drifts are about 45 mV in 2.5 h.

Then, the LD and the QPD were tested together. The beam splitter was turned clockwise by 90° so as to let the laser beam directly project onto the QPD without passing through the collimator lens. Four voltage signals from the QPD were connected to the data acquisition card and the change of ($V_A + V_B - V_C - V_D$) was recorded in ordinary environment. The result is shown in Fig. 11, with about 12 mV in 2.5 h.

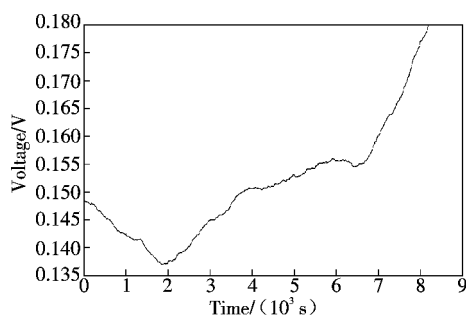


Fig. 10 Result of the circuit in ordinary environment

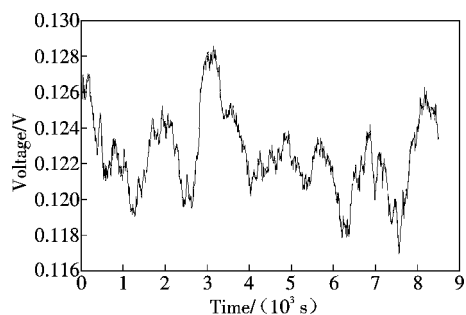


Fig. 11 Result of the LD and QPD in ordinary environment

From the above experiments, it can be seen that although the temperature influence causes the signal drifts of the circuit, the LD and the QPD, the drifts are very small. It can be inferred that most of the drifts of the angle measurement system are caused by the mechanical components and structure, which means that the mechanical components and structure of the angle measurement system are much more sensitive to temperature than the optical and electronic components of the probe.

In addition to temperature change, there are also some minor instable factors, such as vibration and electromagnetic interference. We can also find a clear periodicity from Fig. 9. The stability can be improved further by eliminating the periodic errors so as to increase the signal to noise ratio (SNR).

The voltage range of the angle sensor is about 14 V corresponding to the probe's measuring range of $20 \mu\text{m}$, as shown in Fig. 12. The sensitivity is about 1.43 nm/mV . From Fig. 8 and Fig. 9, the drift of the probe within and without temperature control can be calculated, as listed in Tab. 1. From Tab. 1, it can be concluded that the probe's stability on the X - Y plane within the temperature controlled environment can achieve the standard deviation of 30 nm.

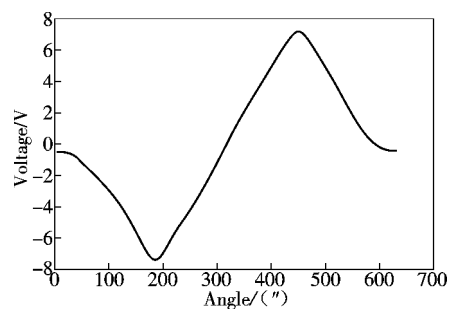


Fig. 12 Characteristic curve of the angle sensor

Tab. 1 Probe's drift in X - Y plane

Time/h	Without the temperature controlled environment		Within the temperature controlled environment	
	Drift/mV	Equivalent displacement/nm	Drift/mV	Equivalent displacement/nm
1.0	700	1 001	20	28.6
2.5	1 300	1 859	30	42.9

2.2.2 Resolution test and analysis

The stability of the 2D angle sensor's output signals determines the probe's resolution. The voltage range of

the 2D angle sensor is about 14 V, as shown in Fig. 12. Corresponding to the probe's measurement range of 20 μm , it is easy to calculate that the required voltage resolution of 1 nm is 0.7 mV. Fig. 13 shows one of the 2D angle sensor's output signals processed only by hardware filter. The noise is up to 50 mV. Fig. 14 shows the signals in Fig. 13 further processed by the sliding average filter with the sliding window size of 50 points. The drift reduces to only 14 mV in nearly 1 h. From Fig. 14, it can also be seen that the local voltage difference between any two adjacent points is less than 0.6 mV, which means that the change of the equivalent displacement of the probe in X - Y plane in any 5 s is less than 1 nm. Therefore, the angle sensor is stable enough to accomplish a resolution of 1 nm.

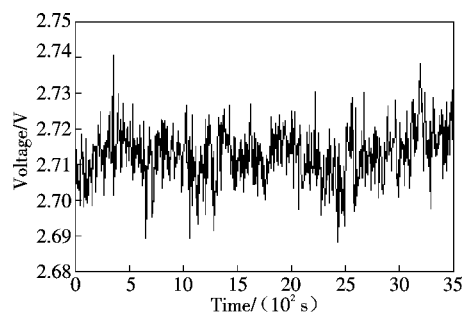


Fig. 13 Signal processed only by hardware filter

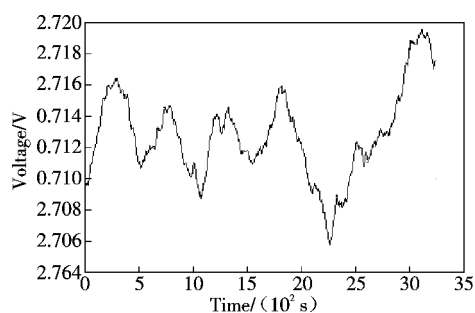


Fig. 14 Signal processed by sliding average filter

2.3 Experiments of the Michelson interferometer

The Michelson interferometer outputs two orthogonal sinusoidal signals with $\pi/2$ phase shift. Experimental results without and within temperature controlled environment are shown in Fig. 15 and Fig. 16, respectively.

The two signals shown in Fig. 15 keep changing for the duration of about 10 h with phase difference changing by at least 2π , which means that the optical path difference between the reference mirror and the object mirror

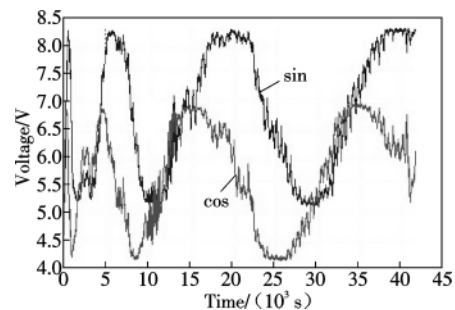


Fig. 15 Results of the interferometer in ordinary environment

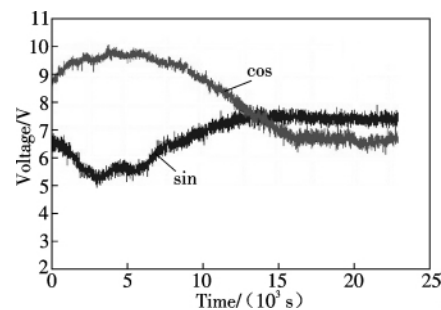


Fig. 16 Results of the interferometer within the constant temperature chamber

has changed by at least $\lambda/2$. In other words, the Michelson interferometer system will drift about 316.4 nm (the wavelength of the LD is 632.8 nm) in about 10 h. However, the two signals shown in Fig. 16 have little fluctuation after 4 h when the temperature is controlled within $(20 \pm 0.025)^\circ\text{C}$.

From the results of Fig. 15 and Fig. 16, it can be concluded that temperature is the primary factor in affecting the stability of the probe in Z direction. Therefore, before measuring, we have to wait for at least 4 h until the temperature in chamber is stable at $(20 \pm 0.025)^\circ\text{C}$.

With the pulse counting and the phase subdivision techniques, the resolution of the Michelson interferometer can be resolved to 1 nm. The probe's stability in the Z direction within the temperature controlled environment can achieve the standard deviation of 30 nm.

3 Conclusion

The stability of a high accuracy contact scanning probe for micro/nano CMM is investigated and analysed in this paper. Experiments were conducted without and within a temperature controlled environment. It is shown

that environmental temperature is the primary factor in affecting the stability of the probe. The mechanical components and structure of the probe are much more sensitive to temperature fluctuation than the optical and electronic components. The probe can meet the resolution of 1 nm and the standard deviation of 30 nm as long as it is put into a temperature controlled environment for at least 4 h before measurement.

References:

- [1] McKeown P. Nanotechnology—Special article [C] // *Nano-Metrology in Precision Engineering*. Hong Kong, China, 1998: 5-55.
- [2] Küng A, Meli F, Thalmann R. Ultraprecision micro-CMM using a low force 3D touch probe [J]. *Meas Sci Technol*, 2007, 18(2): 319-327.
- [3] Peggs G N, Lewis A J, Oldfield S. Design for a compact high-accuracy CMM [J]. *CIRP Annals—Manufacturing Technology*, 1999, 48(1): 417-420.
- [4] Haitjema H, Pril W O, Schellekens P H J. Development of a silicon-based nanoprobe system for 3-D measurements [J]. *CIRP Annals—Manufacturing Technology*, 2001, 50(1): 365-368.
- [5] Ji H, Hsu H Y, Kong L X, et al. Development of a contact probe incorporating a Bragg grating strain sensor for nano coordinate measuring machines [J]. *Meas Sci Technol*, 2009, 20(9): 095304.
- [6] Tibrewala A, Phataralaoha A, Buttgenbach S. Development, fabrication and characterization of a 3D tactile sensor [J]. *Journal of Micromechanics and Microengineering*, 2009, 19(12): 125005.
- [7] Hermann G, Santha C. Design of tactile measuring probes for coordinate measuring machines [J]. *Acta Polytechnica Hungarica*, 2009, 6(1): 63-77.
- [8] Chu C L, Chiu C Y. Development of a low-cost nanoscale touch trigger probe based on two commercial DVD pick-up heads [J]. *Meas Sci Technol*, 2007, 18(7): 1831-1842.
- [9] Fan K C, Cheng F, Wang W L, et al. A scanning contact probe for a micro coordinate measuring machines (CMM) [J]. *Meas Sci Technol*, 2010, 21(5): 054002.
- [10] Cheng Fang, Fan Kuangchao, Fei Yetai. Measurement of pre-travel distance of a touch probe for nano-CMM [J]. *Nanotechnology and Precision Engineering*, 2010, 8(2): 107-113.
- [11] Eom S I, Takaya Y, Hayashi T. Novel contact probing method using single fiber optical trapping probe [J]. *Precision Engineering*, 2009, 33(3): 235-242.
- [12] Claverley J D, Leach R K. A vibrating micro-scale CMM probe for measuring high aspect ratio structures [J]. *Microsystem Technologies*, 2010, 16(8/9): 1507-1512.
- [13] Michihata M, Takaya Y, Hayashi T. Nano position sensing based on laser trapping technique for flat surfaces [J]. *Meas Sci Technol*, 2008, 19(8): 084013.
- [14] Fan K C, Chu C L, Mou J I. Development of a low-cost autofocus probe for profile measurement [J]. *Meas Sci Technol*, 2001, 12(12): 2137-2146.
- [15] Li R J, Fan K C, Tao S, et al. Design of an analogue contact probe for nano-coordinate measurement machines (CMM) [C] // *7th International Symposium on Precision Engineering Measurements and Instrumentation*. Yunnan, China, 2011: 832114.
- [16] Zhang H, Fan K C, Wang J. System design and simulation of constant temperature box using semiconductor refrigeration device [J]. *Journal of Computer Applications in Technology*, 2010, 37(2): 146-152.